VOL. 46
NO. 4
APRIL
2013

JCEJ

JOURNAL OF CHEMICAL ENGINEERING OF JAPAN

[VOL. 46, NO. 4, APRIL 2013]

SCEJ
The Society of Chemical Engineers, Japan

JCEJAQ 46(4)
255-334(2013)
ISSN 0021-9592

Journal of Chemical Engineering of Japan, Vol. 46, No. 4, pp. 279–293, 2013 **Research Paper**

An Extended Method of Simplified Decoupling for Multivariable Processes with Multiple Time Delays

Truong Nguyen Luan Vu[1] and Moonyong Lee[2]

[1] *Faculty of Mechanical Engineering, University of Technical Education Ho Chi Minh City, Ho Chi Minh City 70000, Vietnam*
[2] *School of Chemical Engineering, Yeungnam University, Kyongsan 712–749, South Korea*

Keywords: Decoupling Control, Simplified Decoupling, PI/PID Controller, Dynamic Relative Gain Array, Coefficient Matching Method

A simplified decoupling method is compactly extended for general $n \times n$ multivariable processes by introducing coefficient matching to obtain a stable, proper, and causal simplified decoupler. This simplified decoupling technique allows transfer functions of decoupled apparent processes to be expressed as a set of n equivalent independent processes and then derived as a ratio of the original open-loop transfer function to the diagonal element of the dynamic relative gain array. The advanced design of proportional-integral/proportional-integral derivative (PI/PID) controllers is then directly employed to enhance the overall performance of the decoupling control system while avoiding difficulties arising from properties inherent to simplified decoupling. The structured singular value theory is considered to ensure robust stability of decoupling control systems under multiplicative output uncertainty. Some industrial processes are considered to demonstrate the simplicity and effectiveness of the proposed method.

Introduction

The intricate coupling between many measurement and control signals leads to complex interactions between input and output variables, which complicate the design of multi-loop proportional-integral/proportional-integral derivative (PI/PID) controllers for multivariable processes with multiple time delays. Since the controllers interact with each other, each loop cannot be tuned independently (i.e., adjusting the controller of one loop significantly affects the performance of the other loops and can destabilize the entire control system). Decentralized (multi-loop) or centralized control schemes are usually adopted to address these interactions. For controlling multivariable processes with modest interactions that are closely decoupled, multi-loop PI/PID controllers are usually employed because of their effectiveness, simplicity, failure-tolerant structure, and satisfactory performance (Luyben, 1986; Campo and Morari, 1994; Lee *et al.*, 2004; Truong and Lee, 2010a, 2010b). However, they often perform poorly when the interactions are significant. In such cases, centralized (fully cross-coupled multivariable) PID controllers are advisable. The centralized control approach can be classified into two kinds: a pure centralized strategy (Wang *et al.*, 2003) and a decoupling network combined with multi-loop controllers. Owing to their attractive features, decoupling networks with multi-loop PI/PID controllers have been of significant interest in both academia and industry. Numerous decoupling schemes have been developed and explored (Luyben, 1970; Waller, 1974; Wade, 1997; Åström *et al.*, 2002; Cai *et al.*, 2008; Shen *et al.*, 2010; Garrido *et al.*, 2011), though most consider only two-input, two-output (TITO) systems with dynamic decoupling. However, many multivariable processes studied in control theory and employed in industry consist of more than two inputs and outputs.

Dynamic decoupling control methodologies are available for ideal decoupling, simplified decoupling, and inverted decoupling, with the choice of decoupling method depending largely on each method's advantages and restrictions (McAvoy, 1983; Seborg *et al.*, 1989; Gagnon *et al.*, 1998). Ideal decoupling facilitates convenient controller design because decoupled apparent processes are systematically obtained as a diagonal matrix of processes, but it is rarely used in practice owing to its complicated decoupling elements, realizability problems, and sensitivity to modeling errors. Inverted decoupling, which is also known as feed-forward decoupling, is rarely implemented, even though it can take into account the saturation of manipulated variables. Similar to ideal decoupling, it is sensitive to modeling errors. Simplified decoupling is most widely used in industrial practice because of its robustness and simple decoupling network (i.e., its diagonal elements are set as unity). However, the decoupled apparent processes are intricate, which hinders controller tuning. Thus far, there has been no concrete formulation of general simplified decoupling for processes beyond a recent case study that was restrictively extended to processes using an interaction compensator as a static compensator (i.e., static decoupler) (Liu *et al.*, 2006).

The objective of this study is to derive a general, compact structure for simplified dynamic decoupling by considering the properties of both simplified decoupling and the in-

Received on September 25, 2012; accepted on January 12, 2013
DOI: 10.1252/jcej.12we213
Correspondence concerning this article should be addressed to M. Lee (E-mail address: mynlee@yu.ac.kr).

verted matrix. Decoupled apparent processes can be exactly determined from the ratio of the original open-loop transfer functions and the diagonal elements of the dynamic relative gain arrays (DRGAs), with an essential reduction technique introduced to obtain realizable decoupler elements. An effective method of PI/PID controller design is then suggested for simplified decoupling control systems, where the controllers can be directly obtained without any approximation of the decoupled apparent processes.

The effectiveness of the proposed method is demonstrated through several examples of interacting multivariable processes. Simulation results show that the proposed method consistently performs better than other existing methods, especially for diagonal dominance processes.

1. Extended Simplified Decoupling Design

Consider the block diagram of a decoupling control system for an $n \times n$ stable process in **Figure 1**, where $\tilde{\mathbf{G}}$ denotes a multi-loop controller, and $\mathbf{D}$, a decoupling matrix. $\mathbf{G}$ and $\tilde{\mathbf{Q}}$ are multivariable and decoupled apparent processes, respectively.

The aim of decoupling is to determine a decoupling matrix, $\mathbf{D}$, such that $\mathbf{GD} = \tilde{\mathbf{Q}}$ is diagonal. A multi-loop controller can then be directly designed as a set of n independent SISO processes based on the decoupled apparent process.

$$\begin{bmatrix} g_{11} & \cdots & g_{1n} \\ \vdots & \ddots & \vdots \\ g_{n1} & \cdots & g_{nn} \end{bmatrix} \begin{bmatrix} d_{11} & \cdots & d_{1n} \\ \vdots & \ddots & \vdots \\ d_{n1} & \cdots & d_{nn} \end{bmatrix} = \begin{bmatrix} q_{11} & \cdots & 0 \\ \vdots & \ddots & \vdots \\ 0 & \cdots & q_{nn} \end{bmatrix} \tag{1}$$

From Eq. (1), the two relations below follow:

$$g_{i1}d_{1i} + \cdots + g_{i,i-1}d_{i-1,i} + g_{ii}d_{ii} + g_{i,i+1}d_{i+1,i} + \cdots + g_{in}d_{ni} = q_{ii} \tag{2}$$

$$\begin{bmatrix} g_{11} & \cdots & g_{1,i-1} & g_{1,i} & g_{1,i+1} & \cdots & g_{1,n} \\ \vdots & & \vdots & \vdots & \vdots & & \vdots \\ g_{i-1,1} & \cdots & g_{i-1,i-1} & g_{i-1,i} & g_{i-1,i+1} & \cdots & g_{i-1,n} \\ g_{i+1,1} & \cdots & g_{i+1,i-1} & g_{i+1,i} & g_{i+1,i+1} & \cdots & g_{i+1,n} \\ \vdots & & \vdots & \vdots & \vdots & & \vdots \\ g_{n1} & \cdots & g_{n,i-1} & g_{n,i} & g_{n,i+1} & \cdots & g_{nn} \end{bmatrix} \begin{bmatrix} d_{1i} \\ \vdots \\ d_{i-1,i} \\ d_{i,i} \\ d_{i+1,i} \\ \vdots \\ d_{n,i} \end{bmatrix} = \begin{bmatrix} 0 \\ \vdots \\ 0 \\ 0 \\ \vdots \\ 0 \end{bmatrix} \tag{3}$$

where g_{ij} and d_{ij} denote the (i,j)th elements of $\mathbf{G}$ and $\mathbf{D}$, respectively.

The i-th element of $\tilde{\mathbf{Q}}$ is found by rearranging Eq. (2):

$$\begin{aligned} q_{ii} = g_{ii}d_{ii} + (g_{i1}d_{1i} + g_{i2}d_{2i} + \cdots + g_{i,i-1}d_{i-1,i} \\ + g_{i,i+1}d_{i+1,i} + \cdots + g_{in}d_{ni}) = g_{ii}d_{ii} + \bar{\mathbf{g}}^{ir}\bar{\mathbf{d}}^{ic} \end{aligned} \tag{4}$$

where $\bar{\mathbf{g}}^{ir}$ denotes the i-th row vector of $\mathbf{G}$ dropping the element g_{ii}, i.e., $\bar{\mathbf{g}}^{ir} = [g_{i1}\, g_{i2} \cdots g_{i,i-1} g_{i,i+1} \cdots g_{in}]$, and $\bar{\mathbf{d}}^{ic}$ is the i-th column vector of $\mathbf{D}$, dropping the element d_{ii}, i.e., $\bar{\mathbf{d}}^{ic} = d_{1i}\, d_{2i} \cdots d_{i-1,i} d_{i+1,i} \cdots d_{ni}]^T$.

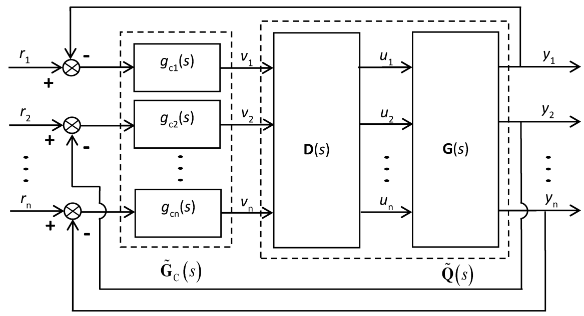

Fig. 1 Block diagram of a decoupling control system

From Eq. (3),

$$\bar{\mathbf{G}}^{i}\bar{\mathbf{d}}^{ic} + \bar{\mathbf{g}}^{ic}d_{ii} = 0 \tag{5}$$

where $\bar{\mathbf{G}}^{i}$ denotes a matrix, dropping the i-th column and row in $\mathbf{G}$, and $\bar{\mathbf{g}}^{ic}$ the i-th column vector of $\mathbf{G}$, dropping the element g_{ii}.

Thus,

$$\bar{\mathbf{d}}^{ic} = -(\bar{\mathbf{G}}^{i})^{-1}\bar{\mathbf{g}}^{ic}d_{ii} \tag{6}$$

From the properties of matrices,

$$\mathbf{G}(\mathrm{adj}\,\mathbf{G}) = |\mathbf{G}|\mathbf{I} \tag{7}$$

where $\mathbf{I}$ denotes the identity matrix, $|\mathbf{G}|$ the determinant of $\mathbf{G}$, and adj $\mathbf{G}$ the adjoint of $\mathbf{G}$. Let $\mathbf{C}$ be the transpose of the matrix of cofactors corresponding to the entries of $\mathbf{G}$:

$$\mathbf{C} = (\mathrm{adj}\,\mathbf{G})^T = \begin{pmatrix} C_{11} & C_{21} & \cdots & C_{n1} \\ C_{12} & C_{22} & \cdots & C_{n2} \\ \vdots & \vdots & \ddots & \vdots \\ C_{1n} & C_{2n} & \cdots & C_{nn} \end{pmatrix}^T \tag{8}$$

Equation (7) implies that

$$g_{i1}C_{i1} + \cdots + g_{i,i-1}C_{i,i-1} + g_{ii}C_{ii} + g_{i,i+1}C_{i,i+1} + \cdots + g_{in}C_{in} = |\mathbf{G}| \tag{9}$$

$$\begin{bmatrix} g_{11} & \cdots & g_{1,i-1} & g_{1,i} & g_{1,i+1} & \cdots & g_{1,n} \\ \vdots & & \vdots & \vdots & \vdots & & \\ g_{i-1,1} & \cdots & g_{i-1,i-1} & g_{i-1,i} & g_{i-1,i+1} & \cdots & g_{i-1,n} \\ g_{i+1,1} & \cdots & g_{i+1,i-1} & g_{i+1,i} & g_{i+1,i+1} & \cdots & g_{i+1,n} \\ \vdots & & \vdots & \vdots & \vdots & & \\ g_{n1} & \cdots & g_{n,i-1} & g_{n,i} & g_{n,i+1} & \cdots & g_{nn} \end{bmatrix} \begin{bmatrix} C_{i1} \\ \vdots \\ C_{i,i-1} \\ C_{i,i} \\ C_{i,i+1} \\ \vdots \\ C_{i,n} \end{bmatrix} = \begin{bmatrix} 0 \\ \vdots \\ 0 \\ 0 \\ \vdots \\ 0 \end{bmatrix} \tag{10}$$

From Eq. (9), the i-th diagonal element of $\mathbf{G}$ can be written as

$$\begin{aligned} g_{ii} = \frac{1}{C_{ii}}[|\mathbf{G}| - (g_{i1}C_{i1} + g_{i2}C_{i2} + \cdots + g_{i,i-1}C_{i,i-1} \\ + g_{i,i+1}C_{i,i+1} + \cdots + g_{in}C_{in})] = \frac{|\mathbf{G}|}{C_{ii}} - \frac{\bar{\mathbf{g}}^{ir}\bar{\mathbf{C}}^{ir}}{C_{ii}} \end{aligned} \tag{11}$$

where $\bar{\mathbf{C}}^{ic} = [C_{i1}\, C_{i2} \cdots C_{i,i-1}\, C_{i,i+1} \cdots C_{in}]^T$. Note that $\bar{\mathbf{C}}^{ic}$ corresponds to the i-th column vector of adj $\mathbf{G}$, dropping the element C_{ii}.

From Eq. (10),

$$\bar{\mathbf{G}}^i\bar{\mathbf{C}}^{ic}+\bar{\mathbf{g}}^{ic}C_{ii}=\mathbf{0} \tag{12}$$

Thus,

$$\bar{\mathbf{g}}^{ic}=-\frac{\bar{\mathbf{G}}^i\bar{\mathbf{C}}^{ic}}{C_{ii}} \tag{13}$$

Substituting Eq. (13) into Eq. (6) gives $\bar{\mathbf{d}}^{ic}$ as

$$\bar{\mathbf{d}}^{ic}=-(\bar{\mathbf{G}}^i)^{-1}\left(-\frac{\bar{\mathbf{G}}^i\bar{\mathbf{C}}^{ic}}{C_{ii}}\right)d_{ii}=d_{ii}\frac{\bar{\mathbf{C}}^{ic}}{C_{ii}} \tag{14}$$

Accordingly, the (j,i)th element of a decoupler can be expressed generally as

$$d_{ji}=d_{ii}\frac{C_{ij}}{C_{ii}},\quad i,j=1,2,\cdots,n;\ j\neq i \tag{15}$$

Substituting Eq. (11) and Eq. (14) into Eq. (4) yields

$$q_{ii}=d_{ii}\frac{|\mathbf{G}|}{C_{ii}} \tag{16}$$

Furthermore, each diagonal element of the DRGA matrix (Witcher and McAvoy, 1977; Bristol, 1979; Skogestad and Poslethwaite, 1996; Truong and Lee, 2010a) can be calculated as:

$$\Lambda_{ii}=[\mathbf{G}\otimes(\mathbf{G}^{-1})^T]_{ii}=g_{ii}\frac{C_{ii}}{|\mathbf{G}|} \tag{17}$$

where Λ_{ii} denotes the i-th diagonal element of the DRGA, and $\otimes$ denotes element-by-element multiplication (the Hadamard or Schur product).

Therefore, from Eq. (15) and Eq. (16), the elements of the decoupled apparent process can be expressed as

$$q_{ii}=d_{ii}\frac{g_{ii}}{\Lambda_{ii}} \tag{18}$$

In order to design simplified decoupling for a stable and square process with n inputs/outputs, all diagonal elements of the decoupling matrix, d_{ii}, are commonly set to unity. This allows the following general forms of the simplified decoupler and the decoupled apparent processes to be respectively given as

$$d_{ji}=\frac{C_{ij}}{C_{ii}},\quad i,j=1,2,\cdots,n;\ j\neq i \tag{19}$$

$$q_{ii}=\frac{g_{ii}}{\Lambda_{ii}} \tag{20}$$

It should be noted that correct input–output (IO) pairing is important in the decoupler design because it may significantly affect the resulting decoupler network and decoupled apparent process, and thus the performance and realizability of the decoupler. In this work, direct pairings are arbitrarily adopted. However, for the other pairing configurations, the same procedure can be applied to the decoupler design once the IO pairing variables are rearranged on the diagonal.

2. Simplified Decoupling Design for Typical Processes

This section analytically develops simplified decoupling for 2×2, 3×3, and 4×4 processes using Eq. (19) and Eq. (20).

2.1 Simplified decoupling for 2×2 processes

Consider a 2×2 system

$$\mathbf{G}=\begin{bmatrix} g_{11} & g_{12}\\ g_{21} & g_{22}\end{bmatrix} \tag{21}$$

The following decoupler matrix results from Eq. (19):

$$\mathbf{D}=\begin{bmatrix} 1 & \dfrac{C_{21}}{C_{22}}\\ \dfrac{C_{12}}{C_{11}} & 1\end{bmatrix} \tag{22}$$

The cofactor of $\mathbf{G}$ is easily given by:

$$\mathbf{C}=(\mathrm{adj}\,\mathbf{G})^T=\begin{bmatrix} C_{11} & C_{12}\\ C_{21} & C_{22}\end{bmatrix}=\begin{bmatrix} g_{22} & -g_{21}\\ -g_{12} & g_{11}\end{bmatrix} \tag{23}$$

and the decoupler elements follow:

$$d_{21}=\frac{C_{12}}{C_{11}}=-\frac{g_{21}}{g_{22}} \tag{24a}$$

$$d_{12}=\frac{C_{21}}{C_{22}}=-\frac{g_{12}}{g_{11}} \tag{24b}$$

The decoupled apparent processes are obtained from Eq. (20):

$$q_{11}=\frac{g_{11}}{\Lambda_{11}}=g_{11}-\frac{g_{12}g_{21}}{g_{22}} \tag{25a}$$

$$q_{22}=\frac{g_{22}}{\Lambda_{22}}=g_{22}-\frac{g_{12}g_{21}}{g_{11}} \tag{25b}$$

These results are in exact agreement with those from most reported approaches for the simplified decoupling of TITO processes.

2.2 Simplified decoupling for 3×3 processes

The transfer function of a 3×3 process is given by

$$\mathbf{G}=\begin{bmatrix} g_{11} & g_{12} & g_{13}\\ g_{21} & g_{22} & g_{23}\\ g_{31} & g_{32} & g_{33}\end{bmatrix} \tag{26}$$

The decoupler matrix is easily obtained from Eq. (19):

$$\mathbf{D}=\begin{bmatrix} 1 & \dfrac{C_{21}}{C_{22}} & \dfrac{C_{31}}{C_{33}}\\ \dfrac{C_{12}}{C_{11}} & 1 & \dfrac{C_{32}}{C_{33}}\\ \dfrac{C_{13}}{C_{11}} & \dfrac{C_{23}}{C_{22}} & 1\end{bmatrix} \tag{27}$$

Table 1 Analytical forms of simplified decoupler elements for some typical processes

Process	Decoupler elements
2×2	$d_{21}=-\frac{g_{21}}{g_{22}},\quad d_{12}=-\frac{g_{12}}{g_{11}}$
3×3	$d_{12}=-\frac{g_{33}g_{12}-g_{32}g_{13}}{g_{33}g_{11}-g_{31}g_{13}},\quad d_{13}=-\frac{g_{22}g_{13}-g_{23}g_{12}}{g_{22}g_{11}-g_{21}g_{12}},\quad d_{21}=-\frac{g_{33}g_{21}-g_{31}g_{23}}{g_{33}g_{22}-g_{32}g_{23}},$ $d_{23}=-\frac{g_{23}g_{11}-g_{21}g_{13}}{g_{22}g_{11}-g_{21}g_{12}},\quad d_{31}=-\frac{g_{31}g_{22}-g_{32}g_{21}}{g_{33}g_{22}-g_{32}g_{23}},\quad d_{32}=-\frac{g_{32}g_{11}-g_{31}g_{12}}{g_{33}g_{11}-g_{31}g_{13}}$
4×4	$d_{12}=\frac{-g_{12}g_{33}g_{44}+g_{12}g_{34}g_{43}+g_{32}g_{13}g_{44}-g_{32}g_{14}g_{43}-g_{42}g_{13}g_{34}+g_{42}g_{14}g_{33}}{g_{11}g_{33}g_{44}-g_{11}g_{34}g_{43}-g_{31}g_{13}g_{44}+g_{31}g_{14}g_{43}+g_{41}g_{13}g_{34}-g_{41}g_{14}g_{33}},$ $d_{13}=\frac{g_{12}g_{23}g_{44}-g_{12}g_{24}g_{43}-g_{22}g_{13}g_{44}+g_{22}g_{14}g_{43}+g_{42}g_{13}g_{24}-g_{42}g_{14}g_{23}}{g_{11}g_{22}g_{44}-g_{11}g_{24}g_{42}-g_{21}g_{12}g_{44}+g_{21}g_{14}g_{42}+g_{41}g_{12}g_{24}-g_{41}g_{14}g_{22}},$ $d_{14}=\frac{-g_{12}g_{23}g_{34}+g_{12}g_{24}g_{33}+g_{22}g_{13}g_{34}-g_{22}g_{14}g_{33}-g_{32}g_{13}g_{24}+g_{32}g_{14}g_{23}}{g_{11}g_{22}g_{33}-g_{11}g_{23}g_{32}-g_{21}g_{12}g_{33}+g_{21}g_{13}g_{32}+g_{31}g_{12}g_{23}-g_{31}g_{13}g_{22}},$ $d_{21}=\frac{-g_{21}g_{33}g_{44}+g_{21}g_{34}g_{43}+g_{31}g_{23}g_{44}-g_{31}g_{24}g_{43}-g_{41}g_{23}g_{34}+g_{41}g_{24}g_{33}}{g_{22}g_{33}g_{44}-g_{22}g_{34}g_{43}-g_{32}g_{23}g_{44}+g_{32}g_{23}g_{43}+g_{42}g_{23}g_{34}-g_{42}g_{24}g_{33}},$ $d_{23}=\frac{-g_{11}g_{23}g_{44}+g_{11}g_{24}g_{43}+g_{21}g_{13}g_{44}-g_{21}g_{14}g_{43}-g_{41}g_{13}g_{24}+g_{41}g_{14}g_{23}}{g_{11}g_{22}g_{44}-g_{11}g_{24}g_{42}-g_{21}g_{12}g_{44}+g_{21}g_{14}g_{42}+g_{41}g_{12}g_{24}-g_{41}g_{14}g_{22}},$ $d_{24}=\frac{g_{11}g_{23}g_{34}-g_{11}g_{24}g_{33}-g_{21}g_{13}g_{34}+g_{21}g_{14}g_{33}+g_{31}g_{13}g_{24}-g_{31}g_{14}g_{23}}{g_{11}g_{22}g_{33}-g_{11}g_{23}g_{32}-g_{21}g_{12}g_{33}+g_{21}g_{13}g_{32}+g_{31}g_{12}g_{23}-g_{31}g_{13}g_{22}},$ $d_{31}=\frac{g_{21}g_{32}g_{44}-g_{21}g_{34}g_{42}-g_{31}g_{22}g_{42}+g_{31}g_{24}g_{42}+g_{41}g_{22}g_{34}-g_{41}g_{24}g_{32}}{g_{22}g_{33}g_{44}-g_{22}g_{34}g_{43}-g_{32}g_{23}g_{44}+g_{32}g_{24}g_{43}+g_{42}g_{23}g_{34}-g_{42}g_{24}g_{33}},$ $d_{32}=\frac{-g_{11}g_{32}g_{44}+g_{11}g_{34}g_{42}+g_{31}g_{12}g_{44}-g_{31}g_{14}g_{42}-g_{41}g_{12}g_{34}+g_{41}g_{14}g_{32}}{g_{11}g_{33}g_{44}-g_{11}g_{34}g_{43}-g_{31}g_{13}g_{44}+g_{31}g_{14}g_{43}+g_{41}g_{13}g_{34}-g_{41}g_{14}g_{33}},$ $d_{34}=\frac{-g_{11}g_{22}g_{34}+g_{11}g_{24}g_{32}+g_{21}g_{12}g_{34}-g_{21}g_{14}g_{32}-g_{31}g_{12}g_{24}+g_{31}g_{14}g_{22}}{g_{11}g_{22}g_{33}-g_{11}g_{23}g_{32}-g_{21}g_{12}g_{33}+g_{21}g_{13}g_{32}+g_{31}g_{12}g_{23}-g_{31}g_{13}g_{22}},$ $d_{41}=\frac{-g_{21}g_{32}g_{43}+g_{21}g_{33}g_{42}+g_{31}g_{22}g_{43}-g_{31}g_{23}g_{42}-g_{41}g_{22}g_{33}+g_{41}g_{23}g_{32}}{g_{22}g_{33}g_{44}-g_{22}g_{34}g_{43}-g_{32}g_{23}g_{44}+g_{32}g_{24}g_{43}+g_{42}g_{23}g_{34}-g_{42}g_{24}g_{33}},$ $d_{42}=\frac{g_{11}g_{32}g_{43}-g_{11}g_{33}g_{42}-g_{31}g_{12}g_{43}+g_{31}g_{13}g_{42}+g_{41}g_{12}g_{33}-g_{41}g_{13}g_{32}}{g_{11}g_{33}g_{44}-g_{11}g_{34}g_{43}-g_{31}g_{13}g_{44}+g_{31}g_{14}g_{43}+g_{41}g_{13}g_{34}-g_{41}g_{14}g_{33}},$ $d_{43}=\frac{-g_{11}g_{22}g_{43}+g_{11}g_{23}g_{42}+g_{21}g_{12}g_{43}-g_{21}g_{13}g_{42}-g_{41}g_{12}g_{23}+g_{41}g_{13}g_{22}}{g_{11}g_{22}g_{44}-g_{11}g_{24}g_{42}-g_{21}g_{12}g_{44}+g_{21}g_{14}g_{42}+g_{41}g_{12}g_{24}-g_{41}g_{14}g_{22}}$

The cofactor of **G** is

$$\mathbf{C}=\begin{bmatrix} C_{11} & C_{12} & C_{13} \\ C_{21} & C_{22} & C_{23} \\ C_{31} & C_{32} & C_{33} \end{bmatrix}=\begin{bmatrix} (g_{33}g_{22}-g_{32}g_{23}) & -(g_{33}g_{21}-g_{31}g_{23}) & -(g_{31}g_{22}-g_{32}g_{21}) \\ -(g_{33}g_{12}-g_{32}g_{13}) & (g_{33}g_{11}-g_{31}g_{13}) & -(g_{32}g_{11}-g_{31}g_{12}) \\ -(g_{22}g_{13}-g_{23}g_{12}) & -(g_{23}g_{11}-g_{21}g_{13}) & (g_{22}g_{11}-g_{21}g_{12}) \end{bmatrix} \tag{28}$$

Hence, the decoupler elements can be analytically found (see **Table 1**).

Equation (20) allows the decoupled apparent processes for the first, second, and third loops to be analytically constituted as:

$$q_{11}=\frac{g_{11}}{\Lambda_{11}}=\left[\frac{g_{11}(g_{22}g_{33}-g_{23}g_{32})-g_{12}(g_{21}g_{33}-g_{23}g_{31})-g_{13}(g_{31}g_{22}-g_{21}g_{32})}{g_{22}g_{33}-g_{23}g_{32}}\right] \tag{29a}$$

$$q_{22}=\frac{g_{22}}{\Lambda_{22}}=\left[\frac{g_{22}(g_{11}g_{33}-g_{13}g_{31})-g_{21}(g_{12}g_{33}-g_{13}g_{32})-g_{23}(g_{32}g_{11}-g_{31}g_{12})}{g_{11}g_{33}-g_{13}g_{31}}\right] \tag{29b}$$

$$q_{33}=\frac{g_{33}}{\Lambda_{33}}=\left[\frac{g_{33}(g_{11}g_{22}-g_{12}g_{21})-g_{31}(g_{13}g_{22}-g_{12}g_{23})-g_{32}(g_{23}g_{11}-g_{13}g_{21})}{g_{11}g_{22}-g_{12}g_{21}}\right] \tag{29c}$$

It is obvious from Eqs. (27) and (29) that the decoupler elements and the decoupled apparent processes increase in complexity as the process size increases. This is a major difficulty associated with simplified decoupling.

2.3 Simplified decoupling for 4×4 processes

The transfer function of a process is given by:

$$\mathbf{G}=\begin{bmatrix} g_{11} & g_{12} & g_{13} & g_{14} \\ g_{21} & g_{22} & g_{23} & g_{24} \\ g_{31} & g_{32} & g_{33} & g_{34} \\ g_{41} & g_{42} & g_{43} & g_{44} \end{bmatrix} \tag{30}$$

The decoupler matrix can be found using the above procedure:

$$\mathbf{D}=\begin{bmatrix} 1 & \frac{C_{21}}{C_{22}} & \frac{C_{31}}{C_{33}} & \frac{C_{41}}{C_{44}} \\ \frac{C_{12}}{C_{11}} & 1 & \frac{C_{32}}{C_{33}} & \frac{C_{42}}{C_{44}} \\ \frac{C_{13}}{C_{11}} & \frac{C_{23}}{C_{22}} & 1 & \frac{C_{43}}{C_{44}} \\ \frac{C_{14}}{C_{11}} & \frac{C_{24}}{C_{22}} & \frac{C_{34}}{C_{33}} & 1 \end{bmatrix} \tag{31}$$

The analytical forms of the decoupling elements are listed in Table 1.

The aforementioned procedure can also be simply applied to derive analytical forms of decoupling elements for other high-dimensional multivariable processes with multiple time delays.

The above equations show that as the order of the process increases, the resulting transfer functions of the decoupler elements become too complicated to be directly used in the design of the decoupling system. Therefore, it is necessary to approximate them suitably in reduced-order models. It should be noted that any reduction technique can be applied to fitting them into the lower-order models.

3. Reduction Technique for Decoupler Realizability

When designing decouplers for any dynamic decoupling structures, realizability must be strictly considered, and the three requirements of being stable, proper, and causal must be satisfied. For simplified decoupling structures, the decoupler elements can be designed more easily than those for ideal decoupling because the diagonal elements are set as unity. However, all off-diagonal elements must also satisfy the three above-mentioned requirements, which are briefly stated as

(i) Causality requires only present and past input values to compute the output. Accordingly, decoupling elements must not involve non-causal time delay.

(ii) A decoupling element is proper if and only if the order of the denominator term is equal to or greater than that of the numerator term.

(iii) Stability occurs if and only if there are no RHP poles.

Accordingly, for TITO processes, decoupler realizability can be easily checked by considering the direct calculations of the G_{12}/G_{11} and G_{21}/G_{22}. For processes involving time delay and non-minimum phase zeros, the resulting decouplers may lead to elements with the prediction term $e^{\theta s}$ and/or RHP poles. To overcome this problem, Wade (1997) introduced an essential approach for inverted decoupling of TITO processes. However, this technique is not applicable to the simplified decoupling of high-dimensional multivariable processes with multiple time delays because the decoupling elements contain sums of the transfer functions, where the dynamics of the decoupling elements is complicated with different signs and different time delays, even if the elements of the system have simple dynamics. To overcome this difficulty, any proper model reduction technique can be utilized to fit the complex dynamics of decoupling elements into suitable low-order models, including, but not limited to, the least squares algorithm, polynomial approximation, Laguerre expansion, and the Gaussian frequency domain approach. In this paper, the coefficient matching (CM) method proposed by Truong and Lee (2010a) is chosen and extended to obtain reduced-order decoupler elements that satisfy the realizability requirements. To illustrate the decoupler design procedure, CM is briefly outlined here.

Decoupler elements given by Eq. (19) can be expanded in Maclaurin series in s as

$$d_{ji}^{\text{eff}}(s)=a_{ji}\left(1+\frac{b_{ji}}{a_{ji}}s+\frac{c_{ji}}{a_{ji}}s^2+\frac{d_{ji}}{a_{ji}}s^3\right)+O(s^4) \tag{32}$$

with polynomial coefficients of

$$a_{ji}=d_{ji}^{\text{eff}}(0) \tag{33b}$$

$$b_{ji}=\left.\frac{\mathrm{d}d_{ji}^{\text{eff}}(s)}{\mathrm{d}s}\right|_{s=0} \tag{33c}$$

$$c_{ji}=\frac{1}{2}\left.\frac{\mathrm{d}^2 d_{ji}^{\text{eff}}(s)}{\mathrm{d}s^2}\right|_{s=0} \tag{33d}$$

$$d_{ji}=\frac{1}{6}\left.\frac{\mathrm{d}^3 d_{ji}^{\text{eff}}(s)}{\mathrm{d}s^3}\right|_{s=0} \tag{33e}$$

Static gain, pure delay, first-order lead/lag, and first-order lead/lag plus time delay dynamics are commonly used representative dynamics of the decoupler elements for decoupling structures because of their simplicity and reasonable performance. As an example, suppose that first-order lead/lag dynamics closely approximates the dynamics of the decoupler element.

$$d^{\text{r\_eff}}=\frac{K_{\text{r}}(\tau_{\text{ra}}s+1)}{\tau_{\text{rb}}s+1} \tag{34}$$

Expanding the reduced dynamics in Eq. (34) as a Maclaurin series in s gives:

$$d^{\text{r\_eff}}(s)=K_{\text{r}}\{1+(\tau_{\text{ra}}-\tau_{\text{rb}})s-(\tau_{\text{ra}}-\tau_{\text{rb}})\tau_{\text{rb}}s^2\}+O(s^3) \tag{35}$$

where K_r, τ_{ra}, and τ_{rb} must be found to approximate d_{ii}^{eff} as closely as possible over the relevant control frequency ranges. Comparing the first, second, and third terms of Eq. (35) with those of Eq. (32) leads to the following explicit

Table 2 Relations between process parameters and polynomial coefficients for typical decoupler models

Cases	Models	Relations
a	K_r	$K_\mathrm{r} = a_{ji}$
b	$\dfrac{K_\mathrm{r}(\tau_\mathrm{ra}s+1)}{(\tau_\mathrm{rb}s+1)}$	$K_\mathrm{r} = a_{ji}$, $\tau_\mathrm{rb} - \tau_\mathrm{ra} = \left(-\dfrac{b_{ji}}{a_{ji}}\right)$; $(\tau_\mathrm{rb} - \tau_\mathrm{ra})\tau_\mathrm{rb} = \left(\dfrac{c_{ji}}{a_{ji}}\right)$
c	$K_\mathrm{r}e^{-\theta_\mathrm{r}s}$	$K_\mathrm{r} = a_{ji}$; $\theta_\mathrm{r} = \left(-\dfrac{b_{ji}}{a_{ji}}\right)$
d	$\dfrac{K_\mathrm{r}(\tau_\mathrm{ra}s+1)e^{-\theta_\mathrm{r}s}}{(\tau_\mathrm{rb}s+1)}$	$K_\mathrm{r} = a_{ji}$, $(\theta_\mathrm{r} + \tau_\mathrm{rb} - \tau_\mathrm{ra}) = \left(-\dfrac{b_{ji}}{a_{ji}}\right)$, $\dfrac{1}{2}\theta_\mathrm{r}^2 + (\theta_\mathrm{r} + \tau_\mathrm{rb} - \tau_\mathrm{ra})\tau_\mathrm{rb} - \tau_\mathrm{ra}\theta_\mathrm{r} = \left(\dfrac{c_{ji}}{a_{ji}}\right)$, $\left(\dfrac{\theta_\mathrm{r}^2}{2} + \tau_\mathrm{rb}\theta_\mathrm{r} + \tau_\mathrm{rb}^2 - \tau_\mathrm{ra}\theta_\mathrm{r} - \tau_\mathrm{ra}\tau_\mathrm{rb}\right)\tau_\mathrm{rb} + \dfrac{\theta_\mathrm{r}^3}{6} - \dfrac{\tau_\mathrm{ra}\theta_\mathrm{r}^2}{2} = \left(-\dfrac{d_{ji}}{a_{ji}}\right)$

equations for K_r, τ_ra, and τ_rb:

$$K_\mathrm{r} = a_{ii} \tag{36a}$$

$$\tau_\mathrm{rb} = -\frac{c_{ii}}{b_{ii}} \tag{36b}$$

$$\tau_\mathrm{ra} \frac{b_{ii}}{a_{ii}} - \frac{c_{ii}}{b_{ii}} \tag{36c}$$

The relationships between the polynomial coefficients and the decoupler element parameters for the other dynamic models are also listed in **Table 2**. These relationships facilitate the calculation of the decoupler element parameters θ_r, τ_ra, and τ_rb.

For the resulting decoupler element to be realizable, the values of θ_r, τ_ra, and τ_rb must be real and positive. This is demonstrated by various case studies that consider Table 2.

Case a: if there are non-realizable elements due to non-causal time delay, RHP poles, and improper decoupler elements, the decoupler elements should be designed as steady-state decoupled process gains to force the non-realizable elements into realizability.

Case b: if there are non-realizable elements due to non-causal time delay, it is recommended to design the decoupler elements using the first-order lead/lag model.

Case c: if there are non-realizable elements due to RHP poles and/or improper decoupler elements, it is recommended to design the decoupler element using the pure delay model.

Case d: if the decoupler elements are realizable, it is recommended to design them using the first-order lead/lag with time delay model.

The proposed reduction technique is simple, comprehensible and easy to implement in practice. It is always possible to choose realizable decoupling elements, but their actual dynamics may be sacrificed to meet the realizability requirements.

It is important to note that the above CM method is effectively used for a square, stable, and diagonal dominance multivariable process with a modest interaction. Otherwise, the CM method must be extended to high-order models with the same procedure or any other techniques (i.e., the above-mentioned reduction techniques) can be utilized to effectively obtain the suitable high-order models that can represent the complex dynamics of decoupler elements.

4. PID Controller Design for Simplified Decoupling

In this study, PI/PID tuning rules are extended by considering those reported by Truong and Lee (2010c) because they have many advantages, including simplicity, robust performance, analytical form, and effectiveness for simplified decoupling systems.

The overall procedure for deriving the tuning rules is as follows:

For the simplified control system, diagonal PI/PID controllers, $\tilde{\mathbf{G}}_\mathrm{C}(s)$, are implemented for the decoupled apparent process, $\tilde{\mathbf{Q}}(s)$. From the standard block diagram of decoupling control (Figure 1), the closed-loop transfer function matrix between the set points and outputs is given as:

$$\tilde{\mathbf{H}}(s) = \tilde{\mathbf{Q}}(s)\tilde{\mathbf{G}}_\mathrm{C}(s)(\mathbf{I} + \tilde{\mathbf{Q}}(s)\tilde{\mathbf{G}}_\mathrm{C}(s))^{-1} = (\tilde{\mathbf{G}}_\mathrm{C}^{-1}(s)\tilde{\mathbf{Q}}^{-1}(s) + \mathbf{I})^{-1} \tag{37}$$

Therefore, the inverse of the matrix is given by

$$\tilde{\mathbf{H}}^{-1}(s) = \tilde{\mathbf{G}}_\mathrm{C}^{-1}(s)\tilde{\mathbf{Q}}^{-1}(s) + \mathbf{I} \tag{38}$$

and the resulting controller can be written as

$$\tilde{\mathbf{G}}_\mathrm{C}(s) = \tilde{\mathbf{Q}}^{-1}(s)(\tilde{\mathbf{H}}^{-1}(s) - \mathbf{I})^{-1} \tag{39}$$

Note that the controller in Eq. (39) is not in standard PI/PID form and it consists of two parts, i.e., $\tilde{\mathbf{Q}}^{-1}(s)$ and $(\tilde{\mathbf{H}}^{-1}(s) - \mathbf{I})^{-1}$.

From Eqs. (16) and (18), when d_{ii} are set to unity, the first part, $\tilde{\mathbf{Q}}^{-1}(s)$, can be written as

$$\tilde{\mathbf{Q}}^{-1}(s)=\operatorname{diag}\left\{\frac{\Lambda_{ii}(s)}{g_{ii}(s)}\right\}=\operatorname{diag}\left\{\frac{C_{ii}}{|\mathbf{G}|}\right\} \tag{40}$$

and $(\tilde{\mathbf{H}}^{-1}(s)-\mathbf{I})^{-1}$ can be expressed as

$$(\tilde{\mathbf{H}}^{-1}(s)-\mathbf{I})^{-1}=\operatorname{diag}\left\{\frac{h_{ii}(s)}{1-h_{ii}(s)}\right\} \tag{41}$$

where h_{ii} is the diagonal element of $\tilde{\mathbf{H}}(s)$ that corresponds to the desired closed-loop transfer function of each loop.

Substituting Eqs. (41) and (40) into Eq. (39) gives:

$$\tilde{\mathbf{G}}_{\mathrm{C}}(s)=\operatorname{diag}\left\{\frac{\Lambda_{ii}(s)}{g_{ii}(s)}\frac{h_{ii}(s)}{1-h_{ii}(s)}\right\}=\operatorname{diag}\left\{\frac{C_{ii}}{|\mathbf{G}|}\frac{h_{ii}(s)}{1-h_{ii}(s)}\right\} \tag{42}$$

Wang (2003) derived the general form of the desired closed-loop transfer function, $h_{ii}(s)$, of the i-th loop by considering the analysis of the characterizations of time delays and non-minimum phase zeros on the decoupling controller:

$$h_{ii}(s)=f_i(s)e^{-L_i s}\prod_{z\in\mathbf{Z}^{+}_{|\mathbf{G}|}}\left(\frac{z-s}{z+s}\right)^{N_{zi}} \tag{43a}$$

where $f_i(s)$ is the i-th loop IMC filter (Morari and Zafiriou, 1989). It is important to note that the time delays and non-minimum phase (RHP) zeros are inherent characteristics of the process that cannot be altered by any feedback controller, and are reflected in Eq. (43a) by $e^{-L_i s}$ and $\Pi_{z\in\mathbf{Z}^{+}_{|\mathbf{G}|}}((z-s)/(z+s))^{N_{zi}}$, respectively. The minimum amount of time delay that the i-th decoupled loop transfer function must contain can be defined as $L_i=[\Theta(|\mathbf{G}|)-\theta_i]$, where $\Theta(|\mathbf{G}|)$ is the time delay that the determinant of the open-loop transfer function matrix contains, and θ_i is defined by $\theta_i=\min_{j\in\mathbf{J}_i}[\Theta(C_{ij})]$, $\mathbf{J}_i=\{j=1,2,\cdots,n|C_{ij}\neq 0\}$. In addition, $\mathbf{Z}^{+}_{|\mathbf{G}|}$ is the set of all the non-minimum phase zeros of $|\mathbf{G}|$. The characterization on non-minimum phase zeros are given by $N_{zi}=N_z(|\mathbf{G}|)-N_i(z)$, where $N_z(|\mathbf{G}|)$ denotes the non-minimum phase zeros at $s=z$ in $|\mathbf{G}|$ and $N_i(z)$ is specified by the following equation, $N_i(z)=\min_{j\in\mathbf{J}_i}N_z(C_{ij})$.

For a simple process with smallest time delays in the diagonal elements and no RHP zero, the desired closed-loop transfer function can then be chosen simply as

$$h_{ii}(s)=\frac{e^{-\theta_{ii}s}}{(\lambda_i s+1)^{m_i}} \tag{43b}$$

where θ_{ii} denotes the time delay of the i-th diagonal element of the process transfer function matrix. The IMC filter time constant, λ_i, which is also equivalent to the closed-loop time constant, is an adjustable parameter controlling the tradeoffs between performance and robustness. m_i is the relative order of the numerator and denominator in $g_{ii}(s)$.

For instance, substituting Eq. (43b) into Eq. (42) gives the i-th loop controller as

$$g_{ci}(s)=\frac{C_{ii}}{|\mathbf{G}|}\left(\frac{e^{-\theta_{ii}s}}{(\lambda_i s+1)^{m_i}-e^{-\theta_{ii}s}}\right) \tag{44}$$

The controller resulting from Eq. (44) is not in standard PI/PID controller form; the following Maclaurin series expansion can generate the PI/PID controller.

The controller resulting from Eq. (44) is rewritten as

$$g_{ci}(s)=s^{-1}p_i(s) \tag{45}$$

where

$$p_i(s)=s\frac{C_{ii}}{|\mathbf{G}|}\left(\frac{e^{-\theta_{ii}s}}{(\lambda_i s+1)^{m_i}-e^{-\theta_{ii}s}}\right) \tag{46}$$

Expanding $g_{ci}(s)$ as a Maclaurin series yields

$$g_{ci}(s)=\frac{1}{s}[p_i(0)+sp_i'(0)+s^2p_i^n(0)+\cdots] \tag{47}$$

where the first three terms constitute the standard PI/PID controller:

$$g_{ci}(s)=\frac{1}{s}(K_{\mathrm{I}i}+sK_{\mathrm{C}i}+s^2K_{\mathrm{D}i}) \tag{48}$$

with K_{1i}, $K_{\mathrm{C}i}$, and $K_{\mathrm{D}i}$ representing the integral, proportional, and derivative terms of the standard PI/PID controller, respectively.

Comparing Eqs. (47) and (48) yields the resulting PI/PID controller parameters

$$K_{\mathrm{C}i}=p_i'(0) \tag{49a}$$

$$K_{\mathrm{I}i}=p_i(0) \tag{49b}$$

$$K_{\mathrm{D}i}=p_i^n(0) \tag{49c}$$

The resulting PI/PID controllers are basically derived in terms of the general form of the apparent decoupled process without any approximations as shown in Eq. (20). Moreover, it can also be successfully applied to the case in which the decoupler network must be approximated to low-order models to avoid realizability problems. It should be noted that the resulting PI/PID controllers from Eqs. (42) and (44) could introduce a further approximation error when the decoupler elements are not properly approximated with the reduced-order model used. Note that the value of the derivative time is sometimes negligible or negative for certain multivariable processes with any value of λ. In this case, use of the PI controller is recommended.

5. Simulation Study

This section considers four examples to demonstrate the performance of the proposed method. For fair comparison, the performance and robustness of the decoupling control system are measured by the following evaluation criteria.

5.1 Integral absolute error index

To evaluate closed-loop performance, the integral absolute error (IAE) criterion is considered. It is defined as:

$$IAE = \int_0^T |e(t)| \mathrm{d}t \tag{50}$$

where $e(t)=r(t)-y(t)$. T is a finite time chosen for the integral approach steady-state value.

5.2 Total variation (*TV*)

To evaluate the magnitude of the manipulated input, the total movement of the control signal is considered as:

$$TV = \sum_{k=1}^{T} |u(k+1) - u(k)| \tag{51}$$

TV is a good measure of the smoothness of controller output and should be small.

5.3 Robust stability analysis

In control system design, nominal models are approximate representations of actual systems. Discrepancies between an actual system and its mathematical representation (nominal model) are referred to as model/plant mismatch (model uncertainty) and may lead to the violation of some performance specification. A control system is stable if the control system is insensitive to variations in the plant's dynamics (including various possible uncertainties) (Doyle *et al.*, 1982; Morari and Zafiriou, 1989; Skogestad and Poslethwaite, 1996; William, 1999). The multiple sources of uncertainty are commonly grouped into a single complex perturbation (multiplicative input/output forms). Either multiplicative input uncertainty or multiplicative output uncertainty can be used for evaluating the robustness of the multivariable control system. In this paper, multiplicative output uncertainty is selected because it is often less restrictive than multiplicative input uncertainty in the case of control performance, since the sensitivity function can be much less sensitive to output uncertainty than input uncertainty (Skogestad and Poslethwaite, 1996). Therefore, robust stability analysis is carried out herein by considering the multiplicative output uncertainty in each of the process parameters simultaneously, as shown in **Figure 2**. It can be expressed as follows:

$$\Pi_O: \quad \mathbf{G}_p(s) = [\mathbf{I} + \mathbf{E}_O(s)]\mathbf{G}(s); \quad \mathbf{E}_O(s) = \mathbf{\Delta}(s)\mathbf{W}_O(s) \tag{52}$$

where $\mathbf{\Pi}_O$ denotes the set of output perturbed process models. $\mathbf{G}_p(s)$ is the $n \times n$ transfer function matrix of the process model as a function of the perturbation of its nominal process model $\mathbf{G}(s)$ due to uncertainty in the multiplicative output, $\mathbf{E}_O(s)$. The magnitude of the perturbation $\mathbf{E}_O(s)$ can be measured in terms of a bound on $\bar{\sigma}(\mathbf{E}_O)$.

$$\bar{\sigma}[\mathbf{E}_O(j\omega)] \le \mathbf{W}_O(j\omega), \quad \forall\omega \tag{53}$$

where the bound (weight) $\mathbf{W}_O(j\omega)$ can also be interpreted as a scalar weight on a normalized perturbation, $\Delta(s)$, with $\bar{\sigma}[\Delta(j\omega)] \le 1$, $\forall\omega$.

The structured singular value (SSV) synthesis, also known as μ-synthesis, suggested by Doyle *et al.* (1982) is employed here to measure the robustness of the control systems. Any perturbation blocks can be rearranged into the general $\mathbf{M}-\Delta$ control structure (Figure 2) where $\Delta(s)$ is the perturbation block with $\bar{\sigma}[\Delta(j\omega)] \le 1$, $\forall\omega$. $\mathbf{M}(s)$ involves all other blocks such as the plant, controller, and weighting factors.

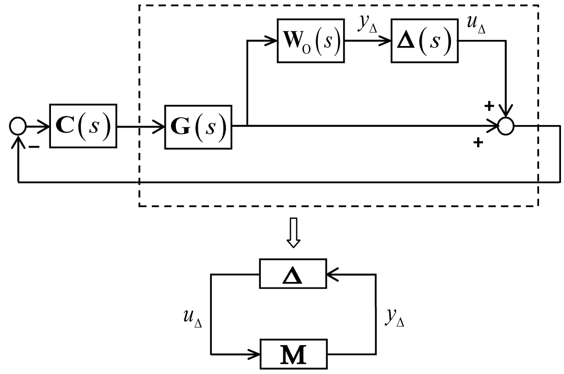

Fig. 2 Control system with multiplicative output uncertainty and its $\mathbf{M}$–$\mathbf{\Delta}$ control structure for robustness analysis

For a multivariable process with multiplicative output uncertainty, the transfer function matrix from the outputs to the inputs of $\Delta(s)$ can be determined by

$$\mathbf{M}(s) = -\mathbf{W}_O(s)\mathbf{G}(s)\mathbf{C}(s)[\mathbf{I} + \mathbf{G}(s)\mathbf{C}(s)]^{-1} \tag{54}$$

where $\mathbf{C}(s)$ denotes the controller.

According to the μ-synthesis, multi-loop control systems will remain stable under multiplicative output uncertainty if the following constraint inequality is satisfied:

$$\mu[\mathbf{M}(j\omega)] = \mu\{\mathbf{W}_O(j\omega)\mathbf{G}(j\omega)\mathbf{C}(j\omega)[\mathbf{I} + \mathbf{G}(j\omega)\mathbf{C}(j\omega)]^{-1}\} < 1, \quad \forall\omega \tag{55}$$

Note that $\mathbf{M}(s)$ and $\Delta(s)$ are required to be stable.

Remarks:

1. $\mu[\mathbf{M}(j\omega)] = 0$. In this situation, no perturbation exists in the multi-loop control system.
2. $\mu[\mathbf{M}(j\omega)] = 1$. There exists a perturbation, with $\bar{\sigma}(\Delta) = 1$, which is just sufficiently large to make $\mathbf{I} - \mathbf{M}(s)\Delta(s)$ singular.
3. A smaller value of $\mu[\mathbf{M}(j\omega)]$ is desirable; larger values allow small perturbations to make $\mathbf{I} - \mathbf{M}(s)\mathbf{\Delta}(s)$ singular.

In order to utilize μ-synthesis for ideal, inverted, and simplified decoupling systems, Eqs. (52), (54), and (55) must be modified by replacing **G** with **GD**.

5.4 Example 1: Wood and Berry (WB) column

A pilot-scale distillation column consisting eight-trays and re-boiler is considered for the separation of methanol and water (Wood and Berry, 1973). The open-loop transfer function matrix is given by

$$\mathbf{G}(s)=\begin{bmatrix}\dfrac{12.8e^{-s}}{16.7s+1} & \dfrac{-18.9e^{-3s}}{21s+1}\\ \dfrac{6.6e^{-7s}}{10.9s+1} & \dfrac{-19.4e^{-3s}}{14.4s+1}\end{bmatrix} \quad (56)$$

The simplified decoupling matrix can easily be obtained using the CM method:

$$\mathbf{D}(s)=\begin{bmatrix}1 & \dfrac{1.477(16.70s+1)e^{-2s}}{21s+1}\\ \dfrac{0.34(14.4s+1)e^{-4s}}{10.9s+1} & 1\end{bmatrix} \quad (57)$$

The design methods of Wang *et al.* (2000) and Truong and Lee (2010c) are compared here as they are found to be superior to other methods. The method of Wang *et al.* (2000) was employed for the simplified decoupling of the TITO system, based on the assumption that the resulting decoupler elements can be represented using the first-order lead/lag plus time delay process model, with the second-order model used for multi-loop PID sequential tuning. Accordingly, the simplified decoupler matrix obtained by Wang *et al.* (2000) is exactly the same as that obtained from the proposed method for this 2×2 process. The design approach suggested by Truong and Lee (2010c) is applied only for the conventional PI multi-loop control system.

For a fair comparison, SSV synthesis is considered for all three control systems by assuming a multiplicative output uncertainty,

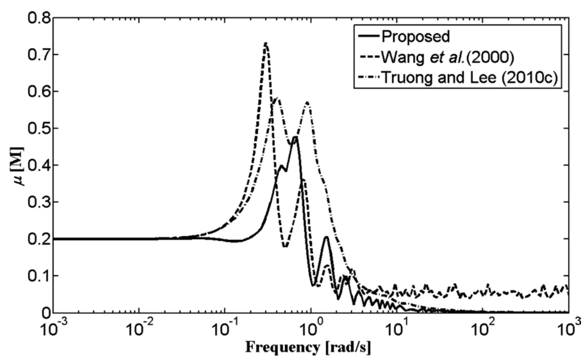

Fig. 3 SSV plots for robust stability in the WB column

$$\mathbf{W}_{\mathrm{O}}(s)=\mathrm{diag}\left\{-\frac{s+0.2}{2s+1},\ -\frac{s+0.2}{2s+1}\right\},$$

that can be physically regarded as relative uncertainty decreasing by up to 50% at high frequencies and by almost 20% in the low frequency range. According to the SSV synthesis for multiplicative output uncertainty, a set of adjustable parameters, λ_i, can be found for the proposed method to achieve the desirable specifications of robust stability and suitable performance by increasing them monotonically. The closed-loop time constant values, λ_i, for loops 1 and 2 are 2.91 and 4.11, respectively. **Figure 3** shows that the maximum value of μ is less than unity, and therefore that the proposed control system guarantees robust stability. Studies of various multi-delay processes have shown that when λ_i values are small, the proposed nominal control system can achieve significant improvements, with small IAE values and fast output responses. However, the robustness of the control system tends to decrease in practice because small perturbations can make $\mathbf{I}-\mathbf{M}(s)\boldsymbol{\Delta}(s)$ singular. Larger values of λ_i systematically provide smaller μ-values. Therefore, the nominal control system will be robust in practice. The trade-off between performance and robustness is considered here to find a set of λ_i that achieve the desirable specifications of robust stability and performance.

The resulting SSV values for the other methods are also shown in Figure 3. The proposed simplified decoupling system is apparently more robust than the others. The resulting controller parameters and performance indices calculated for each method are listed in **Table 3**. **Figure 4** compares the closed-loop time responses of each of the design methods when the unit step changes in the set-points are sequentially made at $t=0$ and $t=80$ to the 1st and 2nd loops, respectively. The figure shows that the proposed design method performs well, with fast and well-balanced responses in comparison with the other methods. Its effectiveness is also confirmed by its *IAE* value in Table 3, which is the smallest.

To demonstrate the robust performance of the proposed method, the controller was investigated by inserting a perturbation uncertainty ±10% in all three parameters, simultaneously, whereas the controller settings were those provided for the nominal process. The simulation results of the model mismatch for various tuning methods are given in **Table 4**. The proposed method shows more robust performance than the above-mentioned methods.

Table 3 Controller parameters and resulting performance indices for the WB column

Tuning methods	Loops	K_C	τ_I	τ_D	λ	$\mu(\mathbf{M})$	*TV*	*IAE*
Proposed	1	0.400	9.964	—	2.910	0.479	1.629	12.297
	2	−0.119	8.169	—	4.110			
Wang *et al.* (2000)	1	0.216	2.853	0.081	—	0.734	0.882	14.336
	2	−0.068	3.516	0.939	—			
Truong and Lee (2010c)	1	0.749	10.073	—	1.110	0.584	1.646	22.12
	2	−0.082	7.981	—	7.110			

IAE: total sum of each loop's IAE_i. *TV*: total sum of each loop's TV_i.

5.5 Example 2: Vinante and Luyben (VL) column

A 24-tray tower separating a mixture of methanol and water, studied by Luyben (1986), has the following transfer function matrix

$$\mathbf{G}(s)=\begin{bmatrix}\dfrac{-2.2e^{-s}}{7s+1} & \dfrac{1.3e^{-0.3s}}{7s+1}\\ \dfrac{-2.8e^{-1.8s}}{9.5s+1} & \dfrac{4.3e^{-0.35s}}{9.2s+1}\end{bmatrix} \quad (58)$$

In accordance with Eq. (24b), d_{12} is the non-realizable element due to non-causal time delay (i.e., $d_{12}=0.591e^{0.7s}$). Therefore, d_{12} must be designed as steady-state decoupled process gains to make the non-realizable elements realizable. The simplified decoupling matrix is then obtained using the CM method:

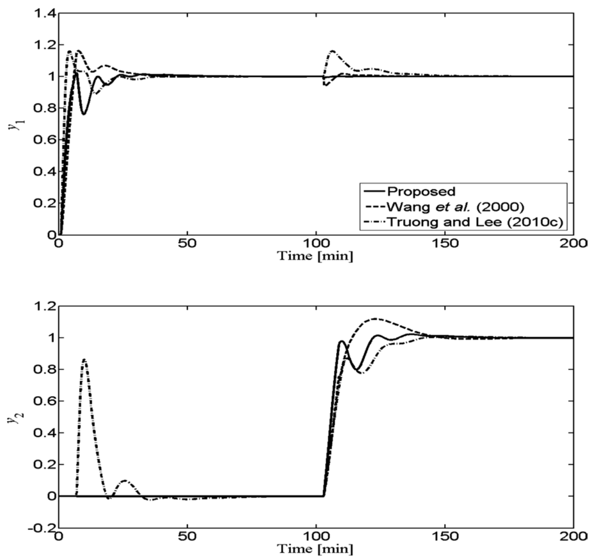

Fig. 4 Closed-loop responses to sequential step changes in the set-points for the WB column

$$\mathbf{D}(s)=\begin{bmatrix}1 & 0.591\\ \dfrac{0.651(9.2s+1)e^{-1.45s}}{9.5s+1} & 1\end{bmatrix} \quad (59)$$

Furthermore, since the process has no RHP zeros but $\theta_{11}>\theta_{12}$, the desired closed-loop transfer function has to be designed using Eq. (43a) as $h_{11}(s)=e^{-s}/(\lambda_1 s+1)$ and $h_{22}(s)=e^{-1.05s}/(\lambda_2 s+1)$.

The performance of the proposed method was compared with that of the ideal decoupling Cai *et al.* (2008) and Truong and Lee (2010c) methods, whereas the ideal decoupling matrix is given by

$$\mathbf{D}(s)=\begin{bmatrix}\dfrac{89.87s+9.46}{25.116s^2+59.112s+5.82} & \dfrac{53.105s+5.59}{25.116s^2+59.112s+5.82}\\ \dfrac{-42.504s^2+52.052s+6.16}{25.116s^2+59.112s+5.82} & \dfrac{89.87s+9.46}{25.116s^2+59.112s+5.82}\end{bmatrix} \quad (60)$$

In the simulation study, SSV synthesis is considered for all three control systems, which include the proposed, simplified, and normalized decoupling (Cai *et al.*, 2008) methods, by assuming a multiplicative output uncertainty,

$$\mathbf{W}_{\mathrm{O}}(s)=\operatorname{diag}\left\{-\frac{s+0.2}{2s+1},\ -\frac{s+0.2}{2s+1}\right\}.$$

The $\lambda_{1,2}$ values of the proposed method were chosen to obtain $\mu(\mathbf{M})=0.279$, which gives a higher robustness level than the others. The resulting controller parameters and performance indices are listed in **Table 5**.

Figure 5 shows the closed-loop responses by all the compared methods, wherein the unit step set set-point changes were sequentially introduced into the individual loops. Superior performance of the proposed controller is apparent from the figure and Table 5.

Table 4 Robustness analysis for WB column under ±10% parametric uncertainty in all parameters

	WB (+10)		WB (−10)	
	TV	*IAE*	*TV*	*IAE*
Proposed	1.793	13.710	1.518	13.549
Wang *et al.* (2000)	0.993	16.203	0.898	14.680
Truong and Lee (2010c)	1.890	22.394	1.455	22.852

Table 5 Controller parameters and resulting performance indices for the VL column

Tuning methods	Loops	K_C	τ_I	τ_D	λ	$\mu(\mathbf{M})$	*TV*	*IAE*
Proposed	1	−2.885	6.638	—	0.70	0.279	7.770	3.752
	2	2.144	8.223	—	0.40			
Ideal decoupling	1	−1.666	7.000	—	—	0.792	8.079	7.056
	2	1.067	9.198	—	—			
Truong and Lee (2010c)	1	−1.660	6.516	—	1.90	0.792	3.144	6.239
	2	3.499	8.609	—	0.58			

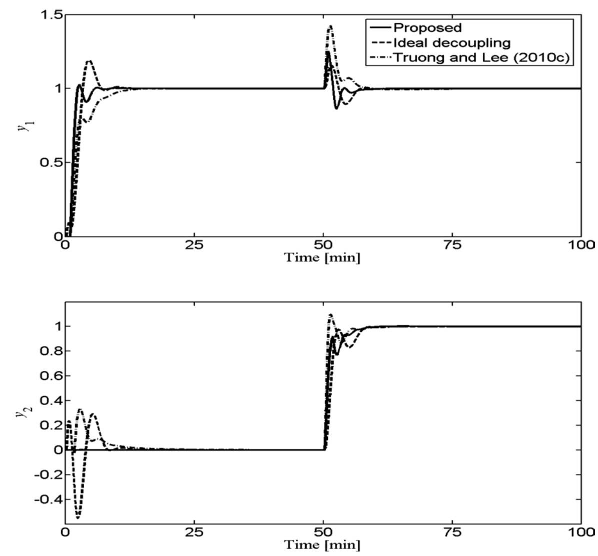

Fig. 5 Closed-loop responses to sequential step changes in the set-points for the VL column

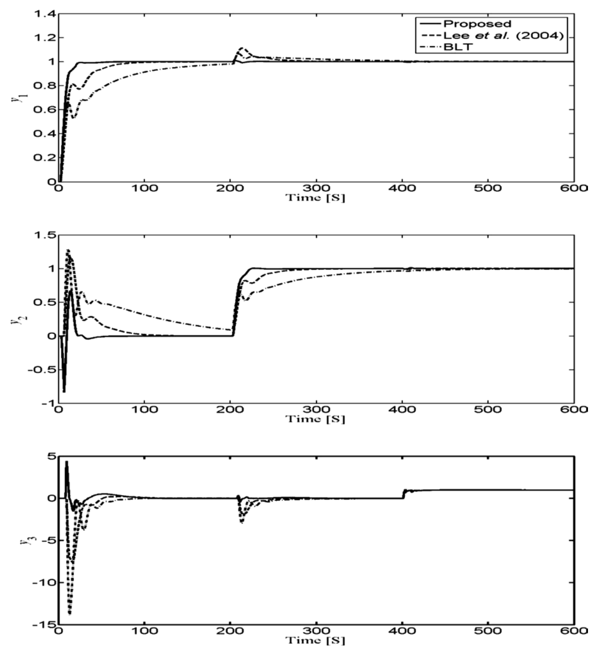

Fig. 6 Closed-loop responses to sequential step changes in the set-points for the OR column

5.6 Example 3: Ogunnaike and Ray (OR) distillation column

A multi-product distillation column for the separation of a binary ethanol-water mixture studied by Ogunnaike *et al.* (1983) is considered. The transfer function matrix is given by Eq. (61).

$$\mathbf{G}(s)=\begin{bmatrix} \dfrac{0.66e^{-2.6s}}{6.7s+1} & \dfrac{-0.61e^{-3.5s}}{8.64s+1} & \dfrac{-0.0049e^{-s}}{9.06s+1} \\ \dfrac{1.11e^{-6.5s}}{3.25s+1} & \dfrac{-2.36e^{-3s}}{5s+1} & \dfrac{-0.01e^{-1.2s}}{7.09s+1} \\ \dfrac{-34.68e^{-9.2s}}{8.15s+1} & \dfrac{46.2e^{-9.4s}}{10.9s+1} & \dfrac{0.87(11.61s+1)e^{-s}}{(3.89s+1)(18.8s+1)} \end{bmatrix} \tag{61}$$

The simplified decoupling matrix is obtained by considering the CM method as follows:

$$\mathbf{D}(s)=\begin{bmatrix} 1 & \dfrac{0.7278(20.463s+1)e^{-1.437s}}{(17.938s+1)} & 0.0048e^{-0.203s} \\ 0.352e^{-0.159s} & 1 & -0.0028 \\ \dfrac{23.238(18.29s+1)e^{-7.2209s}}{(17.271s+1)} & \dfrac{-26.457(4.128s+1)e^{-6.4305s}}{(14.521s+1)} & 1 \end{bmatrix} \tag{62}$$

It is clear from Eq. (61) that the process has no RHP zeros, in accordance with Eq. (43a), the desired closed-loop transfer functions are found as

$$h_{11}(s)=\frac{e^{-2.6s}}{(\lambda_1 s+1)},\quad h_{22}(s)=\frac{e^{-4s}}{(\lambda_2 s+1)},\quad \text{and}\quad h_{33}(s)=\frac{e^{-2.8s}}{(\lambda_2 s+1)}.$$

In the simulation study, the proposed method was compared with those of the BLT (Luyben, 1986), and Lee *et al.*'s method (2004), which are conventional multi-loop PI control systems. For the proposed method and Lee *et al.*'s method (2004), the adjustable parameters λ_i are adjusted to obtain $\mu(\mathbf{M})=0.156$ in order to ensure the same robustness level as that of BLT (Luyben, 1986). The μ-synthesis given by Eq. (55) is considered under the assumption of multiplicative output uncertainty

$$\mathbf{W}_{\mathrm{O}}(s)=\mathrm{diag}\left\{-\frac{s+0.1}{10s+1},\ -\frac{s+0.1}{10s+1},\ -\frac{s+0.1}{10s+1}\right\}$$

for the three control systems. The magnitudes of the sequential step changes in the set-points of loops 1, 2 and 3 were 1, 1, and 1, respectively. **Figure 6** compares the closed-loop responses by the proposed method and those by the BLT (Luyben, 1986) and

Table 6 Controller parameters and resulting performance indices for the OR column

Tuning methods	Loops	K_C	τ_I	τ_D	λ	$\mu(\mathbf{M})$	TV	IAE
Proposed	1	1.383	3.535	—	5.00	0.156	165.36	78.336
	2	−0.148	1.666	—	5.00			
	3	5.00	9.979	—	0.68			
Lee *et al.* (2004)	1	0.672	3.444	—	13.0	0.156	120.58	208.047
	2	−0.140	2.895	—	13.0			
	3	4.725	7.688	—	1.74			
BLT	1	1.51	16.4	—	—	0.156	129.81	671.333
	2	−0.30	18.0	—	—			
	3	2.63	6.61	—	—			

Lee *et al.*'s method (2004). In the figure, one can see that the proposed method has improved output responses over the others. The resulting PI controller parameters together with the performance indices calculated using the above-mentioned methods are summarized in **Table 6**. It is implied that the closed-loop response by the proposed controller shows the smallest total *IAE* among all the compared methods.

5.7 Example 4: HVAC system

Shen *et al.* (2010) introduced the following interactive 4×4 system, the experimental centralized HVAC system of four rooms. The open-loop transfer function matrix is given by:

$$\mathbf{G}(s)=\begin{bmatrix} \frac{-0.098e^{-17s}}{122s+1} & \frac{-0.036e^{-27s}}{149s+1} & \frac{-0.014e^{-32s}}{158s+1} & \frac{-0.017e^{-30s}}{155s+1} \\ \frac{-0.043e^{-25s}}{147s+1} & \frac{-0.092e^{-16s}}{130s+1} & \frac{-0.011e^{-33s}}{156s+1} & \frac{-0.012e^{-34s}}{157s+1} \\ \frac{-0.012e^{-31s}}{153s+1} & \frac{-0.016e^{-34s}}{151s+1} & \frac{-0.102e^{-16s}}{118s+1} & \frac{-0.033e^{-26s}}{146s+1} \\ \frac{-0.013e^{32s}}{156s+1} & \frac{-0.015e^{-31s}}{159s+1} & \frac{-0.029e^{-25s}}{144s+1} & \frac{-0.108e^{-18s}}{128s+1} \end{bmatrix} \quad (63)$$

The simplified decoupling matrix is designed by considering the CM method as follows:

$$\mathbf{D}(s)=\begin{bmatrix} 1 & \frac{-0.341(121.918s+1)e^{-9.151s}}{(146.753s+1)} & \frac{-0.081(132.251s+1)e^{-11.943s}}{(164.976s+1)} & \frac{-0.115(124.604s+1)e^{-8.887s}}{(147.929s+1)} \\ \frac{-0.457(130.872s+1)e^{-8.77s}}{(147.641s+1)} & 1 & \frac{-0.049(235.202s+1)e^{-12.986s}}{(228.983s+1)} & \frac{-0.040(188.514s+1)e^{-14.432s}}{(170.865s+1)} \\ \frac{-0.030(187.930s+1)}{(175s+1)} & \frac{-0.093(97.617s+1)e^{-15.187s}}{(117.144s+1)} & 1 & \frac{-0.304(118.386s+1)e^{-9.165s}}{(145.037s+1)} \\ \frac{-0.049(1946.796s+1)e^{-11.409s}}{(1946.775s+1)} & \frac{-0.073(152.319s+1)e^{-6.741s}}{(166.805s+1)} & \frac{-0.252(124.823s+1)e^{-6.104s}}{(138.501s+1)} & 1 \end{bmatrix} \quad (64)$$

For comparison, the normalized decoupling design suggested by Shen *et al.* (2010) and the inverted decoupling method introduced by Garrido *et al.* (2011) are employed here because of their superiority over other methods.

Shen *et al.*'s normalized decoupling matrix is:

$$\mathbf{D}(s)=\begin{bmatrix} -12.4533e^{-5.9666s} & \frac{(423.3268s+4.5269)e^{-5.4125s}}{121.3755s+1} & \frac{(73.0789+0.8838)e^{-5.4535s}}{113.9022s+1} & \frac{(112.6970s+1.1876)e^{-3.6602s}}{123.5480s+1} \\ \frac{(532.6803s+5.6980)e^{-4.8878s}}{113.8299s+1} & -13.2626e^{-6.3777s} & \frac{52.2751s+0.5300}{113.9022+1} & \frac{49.1501s+0.4144}{123.5480s+1} \\ \frac{40.4368s+0.3752}{113.8299s+1} & \frac{(110.4244s+1.2350)e^{-2.4022s}}{121.3735s+1} & -10.8814e^{-6.7631s} & \frac{(296.1062s+3.1279)e^{-6.6871s}}{123.5480s+1} \\ \frac{(60.8111s+0.6072)e^{-2.4454s}}{113.8299s+1} & \frac{94.9821s+0.9650}{121.9022s+1} & \frac{(264.3081s+2.7412)e^{-5.0369s}}{113.9022s+1} & -10.2987e^{-5.7511s} \end{bmatrix} \quad (65)$$

The inverted decoupling matrix obtained by Garrido *et al.* (2011) is given as the following diagonal and off-diagonal matrices ($\mathbf{D}_d$ and $\mathbf{D}_o$):

$$\mathbf{D}_d(s)=\mathrm{diag}\left\{\frac{-10.2(122s+1)e^{-4.82s}}{113.88s+1}, \frac{-10.87(130s+1)e^{-5.32s}}{121.4s+1}, \frac{-9.8(118s+1)e^{-6.21s}}{113.92s+1}, \frac{-9.26(128s+1)e^{-5.12s}}{123.5s+1}\right\} \quad (66a)$$

$$\mathbf{D}_{\mathrm{o}}(s)=\begin{bmatrix} 0 & \frac{(4.098s+0.036)e^{-5.18s}}{149s+1} & \frac{(1.594s+0.014)e^{-10.2s}}{158s+1} & \frac{(1.935s+0.017)e^{-8.18s}}{155s+1} \\ \frac{(5.219s+0.043)e^{-3.68s}}{147s+1} & 0 & \frac{(1.335s+0.011)e^{-11.7s}}{156s+1} & \frac{(1.456s+0.012)e^{-12.7s}}{157s+1} \\ \frac{(1.367s+0.012)e^{-8.79s}}{153s+1} & \frac{(1.822s+0.016)e^{-11.8s}}{151s+1} & 0 & \frac{(3.759s+0.033)e^{-3.79s}}{146s+1} \\ \frac{(1.606s+0.013)e^{-8.88s}}{156s+1} & \frac{(1.853s+0.015)e^{-7.88s}}{159s+1} & \frac{(3.583s+0.029)e^{-1.83s}}{144s+1} & 0 \end{bmatrix} \quad (66b)$$

For the same degree of robustness, the μ-synthesis given by Eq. (55) is considered under the assumption of multiplicative output uncertainty

$$\mathbf{W}_{\mathrm{O}}(s)=\mathrm{diag}\left\{-\frac{s+0.2}{2s+1},\ -\frac{s+0.2}{2s+1},\ -\frac{s+0.2}{2s+1},\ -\frac{s+0.2}{2s+1}\right\}$$

for the three control systems. This can be physically viewed as the process output measurements from the corresponding sensors decreasing in uncertainty by up to 50% at high frequencies and by almost 20% in the low frequency range. The results in **Figure 7** and **Table 7** show that all the control systems have similarly robust stability. The resulting controller parameters, together with the performance indices calculated for the three methods, are summarized in Table 7.

Figure 8 shows the closed-loop time responses obtained from the same three methods, where the unit step changes in the set points were sequentially made in the individual loops for testing the performance of the control systems.

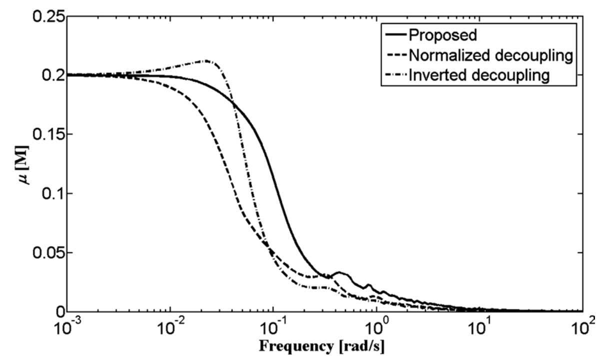

Fig. 7 SSV plots for robust stability in HVAC system

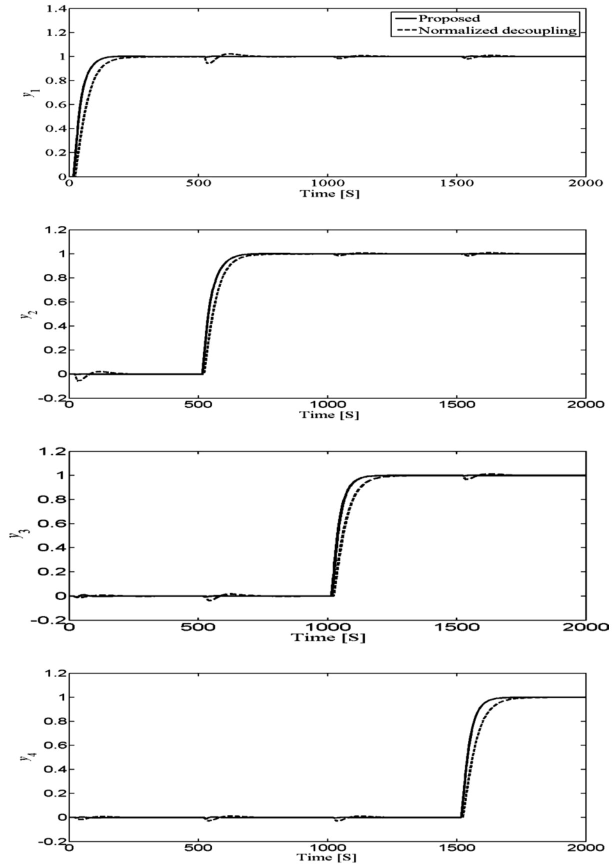

Fig. 8 Closed-loop responses to sequential step changes in the set-points for the HVAC system

Table 7 Controller parameters and resulting performance indices for the HVAC system

Tuning methods	Loops	K_C	τ_I	λ	$\mu(\mathbf{M})$	TV	IAE
Proposed	1	−40.040	112.503	52.0	0.200	267.452	152.679
	2	−40.723	119.774	55.0			
	3	−34.699	114.821	52.0			
	4	−33.122	125.415	57.0			
Normalized decoupling	1	1.639	113.819	—	0.200	196.574	307.031
	2	1.789	121.700	—			
	3	1.611	113.852	—			
	4	1.678	123.412	—			
Inverted decoupling	1	1.639	113.819	—	0.212	219.273	281.875
	2	1.789	121.700	—			
	3	1.611	113.852	—			
	4	1.678	123.412	—			

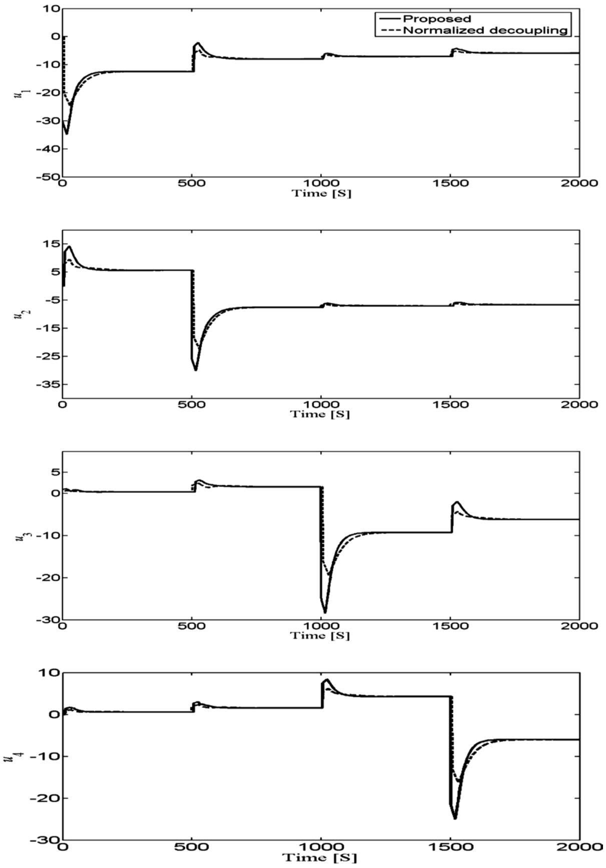

Fig. 9 Controller output responses to the sequential unit step changes in the set-point for the HVAC system

The proposed method demonstrates improved performance, with fast, well-balanced, and smaller settling time responses as well as the smallest *IAE* value in comparison with the other methods. The controller output (manipulated variable) responses are also shown in **Figure 9**. The TV value of the proposed method is larger than those of Shen *et al.* (2010) and Garrido *et al.* (2011), but it is sufficiently smooth for successful operation.

Conclusion

A generalized approach for simplified decoupling was proposed for improving the overall performance of multivariable control systems. Simplified decoupler elements can be compactly formulated as ratios of the (i, j)th cofactors of the open-loop transfer function matrix of a multivariable process to its (i, i)th diagonal elements. Decoupled apparent processes can also easily be expressed as the ratio of the (i, i)th original open-loop transfer function to the (i, i)th diagonal element of the DRGA. Therefore, the resulting PI/PID controllers can be directly used for simplified decoupling systems without any approximations.

Simulation studies were carried out to evaluate the proposed approach. In order to guarantee robustness and ensure a fair comparison, μ-syntheses in the presence of multiplicative output uncertainty were used to measure the degree of robustness.

Simulations were conducted by tuning various controllers of the multivariate processes with multiple time delays. The results indicate that the proposed method consistently performs well with fast and well-balanced closed-loop time responses.

Acknowledgments

This research was supported by the Basic Science Research Program through the National Research Foundation of Korea (NRF), funded by the Ministry of Education, Science and Technology (2012012532), as well as that of University of Technical Education Ho Chi Minh City, Vietnam.

Literature Cited

Åström, K. J., K. H. Johansson and Q. W. Wang; "Design of Decoupled PI Controller for Two-by-Two Systems," *IEE Proc. Contr. Theory Appl.*, **149**, 74–81 (2002)

Bristol, E. H.; "Recent Results on Interactions in Multivariable Process Control," 71st Annual AIChE Meeting, p. 78b, Houston, U.S.A. (1979)

Cai, W. J., W. Ni, M. J. He and C. Y. Ni; "Normalized Decoupling—A New Approach for MIMO Processes Control System Design," *Ind. Eng. Chem. Res.*, **47**, 7347–7356 (2008)

Campo, P. J. and M. Morari; "Achievable Closed-Loop Properties of Systems Under Decentralized Control: Conditions Involving the Steady-State Gain," *IEEE Trans. Automat. Contr.*, **39**, 932–943 (1994)

Doyle, J. C., J. E. Wall and G. Stein; "Performance and Robustness Analysis for Structured Uncertainty," IEEE Conf. Decision and Control, pp. 629–636, Orlando, U.S.A. (1982)

Gagnon, E., A. Pomerleau and A. Desbiens; "Simplified, Ideal or Inverted Decoupling?" *ISA Trans.*, **37**, 265–276 (1998)

Garrido, J., F. Vázquez and F. Morilla; "An Extended Approach of Inverted Decoupling," *J. Process Contr.*, **21**, 55–68 (2011)

Lee, M., K. Lee, C. Kim and J. Lee; "Analytical Design of Multi-Loop PID Controllers for Desired Closed-Loop Responses," *AIChE J.*, **50**, 1631–1635 (2004)

Liu, T., W. Zhang and D. Gu; "Analytical Design of Decoupling Internal Model Control (IMC) Scheme for Two-Input-Two-Output (TITO) Processes with Time Delays," *Ind. Eng. Chem. Res.*, **45**, 3149–3160 (2006)

Luyben, W. L.; "Distillation Decoupling," *AIChE J.*, **16**, 198–203 (1970)

Luyben, W. L.; "Simple Method for Tuning SISO Controllers in Multivariable Systems," *Ind. Eng. Chem. Process Des. Dev.*, **25**, 654–660 (1986)

McAvoy, T. J.; Interaction Analysis: Principles and Applications, Instrument Society of America, Research Triangle Park, U.S.A. (1983)

Morari, M. and E. Zafiriou; Robust Process Control, Prentice Hall, Englewood Cliffs, New Jersey, U.S.A. (1989)

Ogunnaike, B. A., J. P. Lemaire, M. Morari and W. H. Ray; "Advanced Multivariable Control of a Pilot Plant Distillation Column," *AIChE J.*, **29**, 632–640 (1983)

Seborg, D. E., T. F. Edgar and D. A. Mellichamp; Process Dynamics and Control, John Willey & Sons, New York, U.S.A. (1989)

Shen, Y., W. J. Cai and S. Li; "Normalized Decoupling Control for High-Dimensional MIMO Processes for Application in Room Temperature Control HVAC Systems," *Control Eng. Pract.*, **18**, 652–664 (2010)

Skogestad, S. and I. Poslethwaite; Multivariable Feedback Control, John

Wiley and Sons, New York, U.S.A. (1996)
Truong, N. L. V. and M. Lee; "Independent Design of Multi-Loop PI/PID Controllers for Interacting Multivariable Processes," *J. Process Contr.*, **20**, 922–933 (2010a)
Truong, N. L. V. and M. Lee; "Analytical Design of Multi-Loop PI Controllers for Interactive Multivariable Processes," *J. Chem. Eng. Japan*, **43**, 196–208 (2010b)
Truong, N. L. V. and M. Lee; "Multi-Loop PI Controller Design Based on the Direct Synthesis for Interacting Multi-Time Delay Processes," *ISA Trans.*, **49**, 79–86 (2010c)
Wade, H. L.; "Inverted Decoupling: a Neglected Technique," *ISA Trans.*, **36**, 3–10 (1997)
Waller, K. V.; "Decoupling in Distillation," *AIChE J.*, **20**, 592–594 (1974)
Wang, Q. G., B. Huang and X. Guo; "Auto-Tuning of TITO Decoupling Controllers from Step Tests," *ISA Trans.*, **39**, 407–418 (2000)
Wang, Q. G.; Decoupling Control, Springer, Lon Don, U.K. (2003)
Wang, Q. C., T. H. Lee and C. Liu; Relay Feedback: Analysis, Identification and Control, Springer, London, U.K. (2003)
William, S. L.; Control System Fundamentals, CRC Press, Boca Raton, U.S.A. (1999)
Witcher, M. F. and T. J. McAvoy; "Interacting Control Systems: Steady-State and Dynamic Measurement of Interaction," *ISA Trans.*, **16**, 35–41 (1977)
Wood, R. K. and M. W. Berry; "Terminal Composition Control of Binary Distillation Column," *Chem. Eng. Sci.*, **28**, 1707–1717 (1973)